PAPER

Novel Formulation for the Scalar-Field Approach of IE-MEI Method to Solve the Three-Dimensional Scattering Problem

N.M.Alam CHOWDHURY[†a)], ***Student Member***, **Jun-ichi TAKADA**[††], ***and*** **Masanobu HIROSE**[†††], ***Regular Members***

SUMMARY A novel formulation for the Scalar-field approach of Integral Equation formulation of the Measured Equation of Invariance (SIE-MEI) is derived from the scalar reciprocity relation to solve the scalar Helmholtz equation. The basics of this formulation are similar to IE-MEI method for the electromagnetic (EM) problem. The surface integral equation is derived from reciprocity relation and on-surface MEI postulates are used. As a result it generates a sparse linear system with the same number of unknowns as of Boundary Element Method (BEM) and keeps the merits in minimum storage memory requirements and CPU time consumption for computing the final matrix. IE-MEI method has been proposed for two-dimensional (2D) electromagnetic problem, but three-dimensional (3D) problem is very difficult to be extend. This scalar-field approach of IE-MEI method is identical to electromagnetic in 2D, but easily extended to the 3D scalar-field scattering problem contrary to EM problem. The numerical results of sphere and cube are verified with some rigorous or numerical solutions, which give excellent agreement.
key words: *IE-MEI, SIE-MEI, scalar reciprocity relation, 3D acoustic problem, numerical technique for 3D scattering problem*

1. Introduction

The Measured Equation of Invariance (MEI) method has been developed by Mei, Pous et al. [1], [2] for the electromagnetic wave scattering which preserves the advantage of sparse matrix with effective truncation of the mesh boundary near the object surface for the Finite Difference (FD) method. This method can be applied directly on the object surface by using surface integral equation. This Integral Equation formulation of MEI (IE-MEI) was proposed by Rius et al. [3], [4] which preserves the same advantages as MEI, in addition it has same number of unknowns as the conventional Boundary Element Method (BEM) or Method of Moments (MoM). The IE-MEI method has been successfully applied to many electromagnetic (EM) scattering problem by Rius et al. [5]–[7] and Hirose et al. [8]–[11].

IE-MEI method has been used to solve the 2D electromagnetic scattering problem by preserving the sparse linear system, resulting in storage memory and computational time savings as same as MEI method. This method was also applied to 3D scattering problems by Rius et al. [12] and it was found that the accuracy of the solution depends on the choice of metrons and on the geometry of the problem. Recently he concludes [13] that, IE-MEI method is excellent for EM problem of 2D boundaries and not efficient for 3D arbitrary boundaries.

By now, IE-MEI method has been applied only to EM scattering problems. In this paper, we propose an application of IE-MEI method to 3D scalar field problems, such as acoustics. We also describe that 3D extension is simple but effective, which is different from EM scattering problems.

In Scalar-field approach of IE-MEI (SIE-MEI) method, scalar reciprocity relation is first derived from Green's theorem by using 3D scalar Helmholtz equation. Using Hirose's approach [9], the scalar-field integral equation is derived from scalar reciprocity relation which satisfies the MEI postulates [1]. This integral equation is localized and discretized to get the system of linear equations which can be solved with minimum norm solution. For 2D problem, SIE-MEI method is identical to the conventional IE-MEI method for the EM problem, but in 3D case it is simply a scalar-field problem.

This paper is organized as follows. The detailed derivation of scalar-field integral equation is given in Sect. 2. The numerical formulation of SIE-MEI and its boundary value solution are given in Sects. 3 and 4, respectively. Some numerical examples are given in Sect. 5. Finally in Sect. 6, concluding remarks and future extension of this method are presented.

Manuscript received December 27, 2001.
Manuscript revised March 22, 2002.
Final manuscript received April 25, 2002.
[†]The author is with the Department of Electrical & Electronic Engineering, Tokyo Institute of Technology, Tokyo, 152-8552 Japan.
[††]The author is with the Department of International Development Engineering, Tokyo Institute of Technology, Tokyo, 152-8552 Japan.
[†††]The author is with the EM waves division, NMIJ, AIST, Ibaraki-ken, 305-8568 Japan.
a) E-mail: nmalam@mobile.ss.titech.ac.jp

2. Scalar-Field Integral Equation Derived from the Scalar Reciprocity Relation

2.1 Scalar Reciprocity Relation

Let us consider a scalar-field problem in the open space

$$\nabla^2\phi(\boldsymbol{r}) + k^2\phi(\boldsymbol{r}) = -g(\boldsymbol{r}), \quad (1)$$

where ϕ is the scalar field, k is the propagation constant and g is the source distribution.

To derive the reciprocity relation, two separated problems are considered within the same domain as shown in Fig. 1. Then, they are represented by the scalar Helmholtz equations

$$\nabla^2\phi_1(\boldsymbol{r}) + k^2\phi_1(\boldsymbol{r}) = -g_1(\boldsymbol{r}), \quad (2)$$
$$\nabla^2\phi_2(\boldsymbol{r}) + k^2\phi_2(\boldsymbol{r}) = -g_2(\boldsymbol{r}), \quad (3)$$

where ϕ_1 and ϕ_2 are the scalar fields due to the source distribution $g_1(\boldsymbol{r})$ and $g_2(\boldsymbol{r})$, respectively.

These two problems satisfy the following Green's theorem:

$$\int_V \left(\phi_1\nabla^2\phi_2 - \phi_2\nabla^2\phi_1\right) dV = \oint_{\partial V} \left(\phi_1\boldsymbol{\nabla}\phi_2 - \phi_2\boldsymbol{\nabla}\phi_1\right)\cdot d\boldsymbol{S}. \quad (4)$$

Using Eqs. (2) and (3) in Eq. (4), the following *Scalar Reciprocity Relation* is obtained

$$\int_V \left(\phi_2(\boldsymbol{r})g_1(\boldsymbol{r}) - \phi_1(\boldsymbol{r})g_2(\boldsymbol{r})\right) dV = \oint_{\partial V} \left(\phi_1(\boldsymbol{r})\frac{\partial\phi_2(\boldsymbol{r})}{\partial n} - \phi_2(\boldsymbol{r})\frac{\partial\phi_1(\boldsymbol{r})}{\partial n}\right) dS. \quad (5)$$

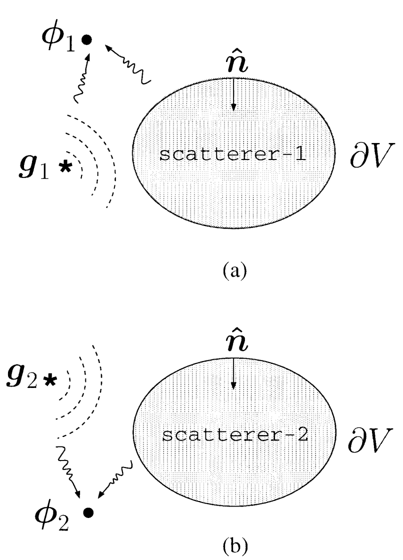

Fig. 1 Scalar-field problems within the same domain.

2.2 Derivation of Integral Equation

Let us consider a closed surface ∂V^+ placed very near to the scatterer-2 which has the same shape as of scatterer-1. Assume that the volume V^+ includes only the source distribution g_2 which produces scalar fields ϕ_2 and $\frac{\partial\phi_2}{\partial n}$ due to the presence of scatterer-2 [9] which are represented by the equivalent monopole source $\rho_2(\boldsymbol{r})$ and the dipole moment $\hat{\boldsymbol{n}}\cdot\boldsymbol{\mu}_2(\boldsymbol{r})$ as shown in Fig. 2. Let ϕ_1 be the scattered field, then $g_1 = 0$ in V^+. Therefore, in the region V^+ there exists scalar field contribution of g_2 and only the scattered field ϕ_1 and its normal derivative $\frac{\partial\phi_1}{\partial n}$ which are produced by the equivalent surface sources of scatterer-1, then the reciprocity relation given in Eq. (5) can be written as

$$\oint_{\partial V^+} \left(\phi_1(\boldsymbol{r})\frac{\partial\phi_2(\boldsymbol{r})}{\partial n} - \phi_2(\boldsymbol{r})\frac{\partial\phi_1(\boldsymbol{r})}{\partial n}\right) dS = -\int_{V^+} \phi_1(\boldsymbol{r})g_2(\boldsymbol{r})dV. \quad (6)$$

Taking the limit $\partial V^+ \to \partial V$ and by rearranging appropriate terms, Eq. (6) reduces to

$$\oint_{\partial V} \left(\phi_1(\boldsymbol{r})\tilde{\rho}_2(\boldsymbol{r}) - \frac{\partial\phi_1(\boldsymbol{r})}{\partial n}\hat{\boldsymbol{n}}\cdot\tilde{\boldsymbol{\mu}}_2(\boldsymbol{r})\right) dS = 0. \quad (7)$$

Equation (7) is the *Scalar-field Integral Equation*, where $\tilde{\rho}_2(\boldsymbol{r}) = g_2(\boldsymbol{r})\Delta w + \frac{\partial\phi_2(\boldsymbol{r})}{\partial n}$ and $\hat{\boldsymbol{n}}\cdot\tilde{\boldsymbol{\mu}}_2(\boldsymbol{r}) = \phi_2(\boldsymbol{r})$ terms represent the equivalent sources near the scatterer. Here Δw is the thickness of the volume source g_2.

3. Formulation of SIE-MEI Method

3.1 SIE-MEI Postulates

Reference to the MEI postulates [1], the scalar-field integral equation (7) is also expected to satisfy the SIE-MEI postulates [14]. These are,

1. local sources exist near the scatterer, and these sources are:
2. dependent on the scatterer geometry,
3. dependent on the position,
4. invariant to the excitation field.

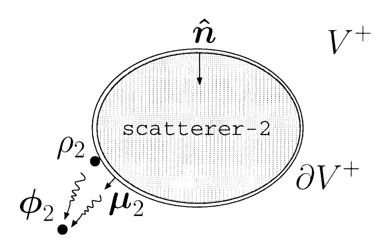

Fig. 2 Surface ∂V^+ very near to the scatterer.

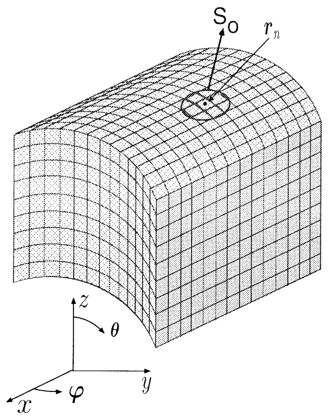

Fig. 3 Arbitrary shaped 3D body.

Here the postulates 1 and 4 reveal that the invariant local sources $\tilde{\rho}_2$ and $\hat{\boldsymbol{n}} \cdot \tilde{\boldsymbol{\mu}}_2$ can be measured from the solutions of scalar-field integral equations, such as ϕ_1 and $\frac{\partial \phi_1}{\partial n}$ with different primary sources. Postulates 2 and 3 reveal that these local sources depend on position and scatterer geometry.

3.2 Localization and Discretization

According to the postulates, let us assume the locally confined sources are essentially non-zero in the local portion, say S_o as shown in Fig. 3, and are zero in the other portion of the scatterer [9].

Hence, Eq. (7) as the localized integral equation

$$\int_{S_0} \left(\phi_1(\boldsymbol{r})\tilde{\rho}_2(\boldsymbol{r}) - \frac{\partial \phi_1(\boldsymbol{r})}{\partial n} \hat{\boldsymbol{n}} \cdot \tilde{\boldsymbol{\mu}}_2(\boldsymbol{r}) \right) dS = 0, \quad (8)$$

which is equivalent to Eq. (2) in Ref. [10].

For the discretization of 3D problem, let us discretize the scatterer surface ∂V and its local portion S_o into N and M segments respectively. Let us expand the local sources $\tilde{\rho}_2$ and $\tilde{\boldsymbol{\mu}}_2$ within S_o centered by $\boldsymbol{r}_n$ into M pulse basis functions as

$$\tilde{\rho}_{2,n}(\boldsymbol{r}) = \sum_{m \in R_n} \tilde{\rho}_{2,n}(\boldsymbol{r}_m) P_m(\boldsymbol{r}), \quad (9)$$

$$\hat{\boldsymbol{n}} \cdot \tilde{\boldsymbol{\mu}}_{2,n}(\boldsymbol{r}) = \sum_{m \in R_n} \hat{\boldsymbol{n}} \cdot \tilde{\boldsymbol{\mu}}_{2,n}(\boldsymbol{r}_m) P_m(\boldsymbol{r}), \quad (10)$$

where $\tilde{\rho}_{2,n}(\boldsymbol{r}_m)$ and $\hat{\boldsymbol{n}} \cdot \tilde{\boldsymbol{\mu}}_{2,n}(\boldsymbol{r}_m)$ are the local sources at $\boldsymbol{r}_m$ and $P_m(\boldsymbol{r})$ is the pulse basis function given by

$$P_m(\boldsymbol{r}) = \begin{cases} 1, & \boldsymbol{r} \text{ is within } m\text{-th segment} \\ 0, & \text{otherwise} \end{cases} \quad (11)$$

and R_n is defined as

$$R_n = \{m_{1,n}, m_{2,n}, \cdots, m_{M,n}\}, \quad (12)$$
$$n = 1, 2, \cdots, N.$$

Substituting Eqs. (9) and (10) into Eq. (8) and interchanging integration and summation, we have

$$\sum_m \left[\tilde{\rho}_{2,n}(\boldsymbol{r}_m) \int_{S_o} \phi_1(\boldsymbol{r}) P_m(\boldsymbol{r}) dS - \hat{\boldsymbol{n}} \cdot \tilde{\boldsymbol{\mu}}_{2,n}(\boldsymbol{r}_m) \int_{S_o} \frac{\partial \phi_1(\boldsymbol{r})}{\partial n} P_m(\boldsymbol{r}) dS \right] = 0. \quad (13)$$

If we assume that ϕ_1 and $\frac{\partial \phi_1}{\partial n}$ are smooth within the segment, then by defining $a_{nm} = \tilde{\rho}_{2,n}(\boldsymbol{r}_m)$ and $b_{nm} = \hat{\boldsymbol{n}} \cdot \tilde{\boldsymbol{\mu}}_{2,n}(\boldsymbol{r}_m)$, Eq. (13) reduces to

$$\sum_m \left[a_{nm}\phi_1(\boldsymbol{r}_m) - b_{nm} \frac{\partial \phi_1(\boldsymbol{r}_m)}{\partial n} \right] = 0. \quad (14)$$

3.3 Derivation of Unknown Coefficients and Sparse Matrix Generation

To obtain a_{nm} and b_{nm} of Eq. (14) the following "measurement" scheme is considered.

For some q-th certain incident field, the secondary source ρ_q is induced to generate the scattered wave for a soft body [15], [17]

$$\phi_{1,q}(\boldsymbol{r}_m) = \oint_{\partial V} \rho_q(\boldsymbol{r}') \, G(\boldsymbol{r}_m, \boldsymbol{r}') \, dS', \quad (15)$$

$$\frac{\partial \phi_{1,q}(\boldsymbol{r}_m)}{\partial n} = \oint_{\partial V} \rho_q(\boldsymbol{r}') \, \frac{\partial G(\boldsymbol{r}_m, \boldsymbol{r}')}{\partial n} \, dS', \quad (16)$$
$$q = 1, 2, \cdots, Q$$

where $G(\boldsymbol{r}_m, \boldsymbol{r}')$ is the three-dimensional free space Green's function, given by

$$G(\boldsymbol{r}_m, \boldsymbol{r}') = \frac{e^{-jkR}}{4\pi R}, \quad (17)$$
$$R = |\boldsymbol{r}_m - \boldsymbol{r}'|.$$

In the practical implementation, ρ_q is explicitly given instead of primary sources, and they are called *metrons* [1].

In matrix form, Eq. (14) becomes

$$[\, \mathbf{C} \; \mathbf{D} \,] \begin{bmatrix} \mathbf{a} \\ \mathbf{b} \end{bmatrix} = 0, \quad (18)$$

where $[\, \mathbf{C} \; \mathbf{D} \,]$ is the $[\, Q \times 2M \,]$ known matrix composed of metron fields and their normal derivatives and $\begin{bmatrix} \mathbf{a} \\ \mathbf{b} \end{bmatrix}$ is the unknown column vector composed of invariant local sources.

The local matrix equation around $\boldsymbol{r}_n$ represented by Eq. (18) is underdetermined (if $Q < 2M$) or overdetermined (if $Q > 2M$) system of linear equations, being dependent on the number of metrons included in the metron set. Whatever the system is, we can solve this linear least square problem with minimum norm solution [16]. Singular Value Decomposition (SVD) is the best choice for this type of solution.

SVD of matrix $[\,\mathbf{C}\ \mathbf{D}\,]$ is expressed as

$$[\,\mathbf{C}\ \mathbf{D}\,] = \mathbf{U}\,\mathbf{\Sigma}\,\mathbf{V}^H, \tag{19}$$

where $\mathbf{U}$ is an Q-by-Q unitary matrix, $\mathbf{V}$ is an $2M$-by-$2M$ unitary matrix, and $\mathbf{\Sigma}$ is an Q-by-$2M$ matrix with diagonal entries σ_j i.e., $\mathbf{\Sigma} = \mathrm{diag}\,\{\sigma_1, \sigma_2, \cdots, \sigma_p\}$, which are nonnegative and arranged in descending order, $\sigma_1 \geq \sigma_2 \geq \cdots \geq \sigma_p \geq 0$, where $p = \min(Q,\, 2M)$.

The first $\min(Q,\, 2M)$ columns of $\mathbf{U}$ and $\mathbf{V}$ are the left and right singular vector of matrix $[\,\mathbf{C}\ \mathbf{D}\,]$ and the smallest singular value of $\mathbf{V}$, is the least square solution of Eq. (18).

Repeat the procedure for each nodal point $n = 1, 2, \cdots, N$ to get the sparse matrices $\mathbf{A}$ and $\mathbf{B}$ which may be the cyclic band matrices (as of Eqs. (16) and (17) in Ref. [14]) or scattered sparse matrices with M nonzero elements in each row which correspond to $\mathbf{a}$ and $\mathbf{b}$ in Eq. (18).

Therefore, the Eq. (14) is represented concisely as

$$\mathbf{A}\,[\,\boldsymbol{\phi}^{\mathrm{sc}}] - \mathbf{B}\,\left[\frac{\partial \boldsymbol{\phi}^{\mathrm{sc}}}{\partial n}\right] \,=\, 0. \tag{20}$$

4. SIE-MEI Method for Soft-Body Problem

As an implementation of SIE-MEI method, let us consider a soft-body problem [17], which satisfies the Dirichlet boundary condition as

$$\phi^{\mathrm{inc}}(\boldsymbol{r}_s) + \phi^{\mathrm{sc}}(\boldsymbol{r}_s) = 0, \qquad \boldsymbol{r}_s \,\in\, \partial V \tag{21}$$

where ϕ^{inc} and ϕ^{sc} are the incident and scattered field, respectively.

Using this condition, Eq. (20) can be expressed as

$$\mathbf{A}\,[\,\boldsymbol{\phi}^{\mathrm{inc}}] + \mathbf{B}\,\left[\frac{\partial \boldsymbol{\phi}^{\mathrm{sc}}}{\partial n}\right] \,=\, 0, \tag{22}$$

where $\frac{\partial \phi^{\mathrm{sc}}}{\partial n}$ is the normal derivative of the scattered field.

Furthermore, the normal derivative of field on the scatterer surface is

$$\frac{\partial \phi(\boldsymbol{r}_s)}{\partial n} = \frac{\partial \phi^{\mathrm{inc}}(\boldsymbol{r}_s)}{\partial n} + \frac{\partial \phi^{\mathrm{sc}}(\boldsymbol{r}_s)}{\partial n}. \tag{23}$$

Using Eq. (22), we have

$$\left[\frac{\partial \boldsymbol{\phi}(\boldsymbol{r}_s)}{\partial n}\right] = \left[\frac{\partial \boldsymbol{\phi}^{\mathrm{inc}}(\boldsymbol{r}_s)}{\partial n}\right] - \mathbf{B}^{-1}\mathbf{A}[\boldsymbol{\phi}^{\mathrm{inc}}(\boldsymbol{r}_s)], \tag{24}$$

which represents the equation of equivalent surface sources on the scatterer.

5. Numerical Examples and Results

As for numerical examples, we considered uniform shape and arbitrary shape 3D convex object. Uniform shape means the body with axial symmetry like sphere, and arbitrary shape means the body with surface singularities like cube.

5.1 General Considerations

Let us consider the scatterer illuminated by the forward directed plane wave

$$\phi^{\mathrm{inc}}(\boldsymbol{r}) \,=\, e^{-j\boldsymbol{k}\,\boldsymbol{\cdot}\,\boldsymbol{r}}, \tag{25}$$

where $\boldsymbol{k}$ is the wave propagation vector, $\boldsymbol{r}$ is the position vector.

Also assume the scattered field generated by the metron

$$\phi^{\mathrm{sc}}(\boldsymbol{r}) \,=\, \oint_{\partial V} \rho(\boldsymbol{r}')\, G(\boldsymbol{r}, \boldsymbol{r}')\, dS', \tag{26}$$

where $\rho(\boldsymbol{r}')$ is the arbitrarily chosen metron to be described more in the next section, $G(\boldsymbol{r}, \boldsymbol{r}')$ is the free space 3D Green's function, and $\boldsymbol{r}$ and $\boldsymbol{r}'$ are the position vectors of observation point and source point, respectively.

Surface discretization is maintained as such that, the segmentation length is approximately one tenth of wavelength. In our observation it gives the good result with minimum number of unknowns N.

Rectangular patch discretization with pulse-basis point-matching method is used to keep the easier mesh generation and minimum number of integration points or nodes which can avoid the extra computational burden. For this type of discretization the possible number of nodes coupled with the local region are 3, 5, 9, etc. The choice of number of segments in the local region depends on the object geometry to get the smooth result.

For accuracy, all the floating point and complex data are taken in double precision in the FORTRAN code.

5.2 The Metron Set

The choice of suitable metron set is an important parameter of this method. Specially for 3D case, without the selection of an appropriate metron set numerical result will not be convergent.

In this paper we propose spherical wave functions [18] as a metron set for 3D scattering problem, which are expressed as

$$\rho(r, \theta, \varphi) = \sum_{n=0}^{\infty} h_n^{(2)}(kr) \sum_{m=-n}^{n} P_n^{|m|}(\cos\theta) e^{jm\varphi}. \tag{27}$$

Here $h_n^{(2)}(kr)$ is the n-th degree outward spherical Hankel function to represent the variation of radial distance r of the object surface, $P_n^{|m|}(\cos\theta)$ is the n-th degree m-th order Associated Legendre function that varies with the polar angle θ, and $e^{jm\varphi}$ is the harmonic function along the equatorial angle φ.

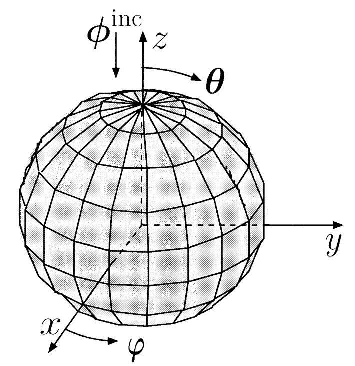

Fig. 4 Plane wave incident on a sphere.

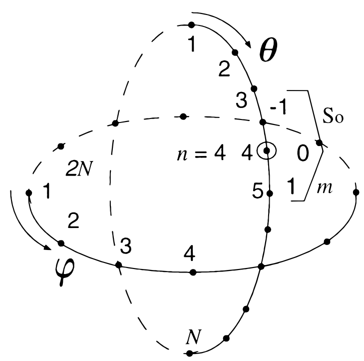

Fig. 5 Localization and discretization of sphere.

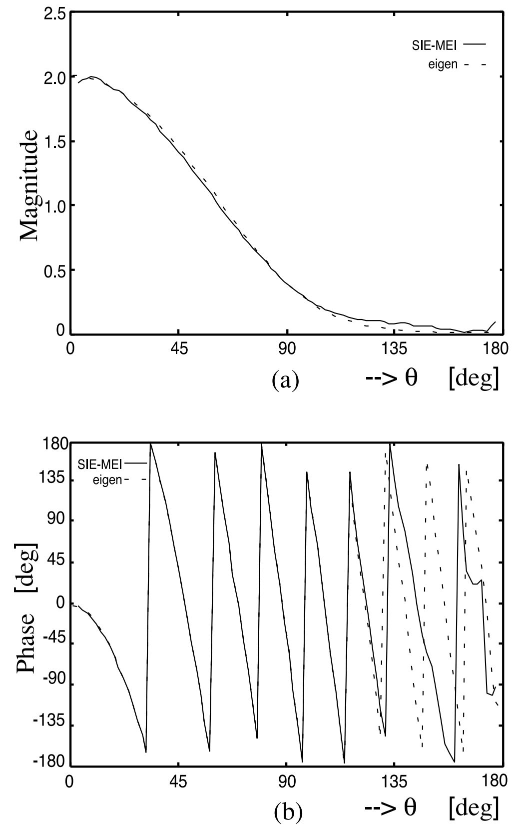

Fig. 6 Equivalent surface source on the sphere (a) magnitude, (b) phase variation.

5.3 Axially Symmetrical Body: Sphere

As for an example of axially symmetrical body, let us consider a sphere as shown in Fig. 4, on which a plane wave is incident from $+z$ direction

$$\phi^{\rm inc}(\boldsymbol{r}) = e^{jka\cos\theta}, \tag{28}$$

where k is the wave propagation number, a is the radius of the sphere and θ is the angle in polar direction.

The problem has the axial symmetry with the surface of constant radial distance. Thus the spherical wave function of Eq. (27) reduces to

$$\rho_q = P_q(\cos\theta), \qquad q = 1, 2, \cdots, Q \tag{29}$$

i.e., the set of *Zonal Harmonics* can be chosen as metron set. Equation (29) is used as local sources in Eq. (26) to get the scattered and its normal derivative field.

For numerical solution the sphere surface S is discretized into N segments in the polar direction θ within the range from 0 to π and $2N$ segments in the azimuthal direction φ within the range from 0 to 2π as shown in Fig. 5. Due to the axial symmetry along φ, measuring function is taken only in θ direction. It is sufficient to discretize the local region S_o into $M = 3$ segments in the polar direction. Azimuthal variation is considered only for the numerical integration of Eq. (26).

Using the above numerical considerations in Eqs. (14) and (24), the equivalent surface source on the sphere can readily be obtained.

The numerical results of equivalent surface source on a sphere using SIE-MEI method is given in Fig. 6. The figure shows the result for a sphere of radius $a = 3$ wavelengths as a function of θ and compares it with the rigorous solution using eigenfunction expansion [17]. The comparison gives the excellent agreement between them except some error in the shadowed region. At this region the phase cannot be calculated accurately due to very small magnitude. But this error is negligible since it does not gives any significant deviation in the scattering computation.

5.4 Arbitrary Shaped Body: Cube

Figure 7 shows a cube as an example of 3D arbitrary shaped body. We consider the same type of plane wave, as Eq. (25), incident on it. As in this problem the surface has polar, azimuthal, and radial variations, Eq. (27) is used as metron set.

Discretization is taken on six faces of the cube and the measuring function is calculated on every segment of all faces. In the measuring operation $M = 5$ segments are considered as the local region S_o as shown in Fig. 8.

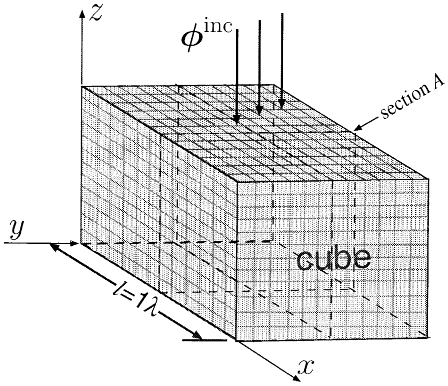

Fig. 7 Plane wave incident on a cube.

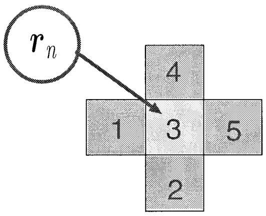

Fig. 8 Segments in the local region with local indexing.

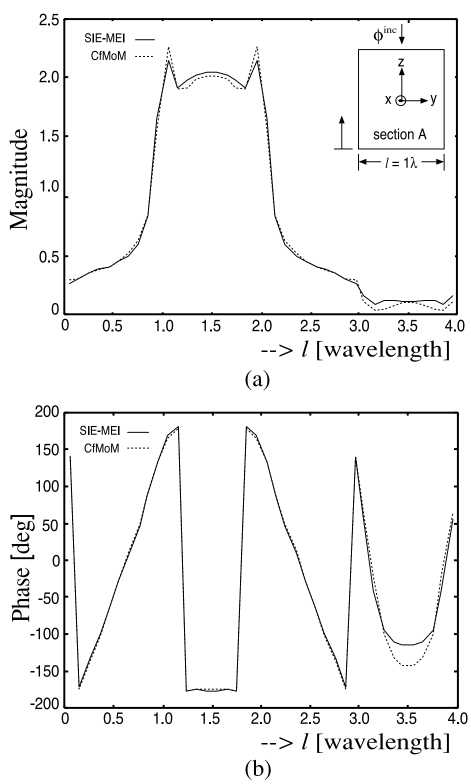

Fig. 9 Equivalent surface source on the Cube (a) magnitude, (b) phase variation.

Figure 9 shows the 2D plot of equivalent surface source on a cube along the perimeter of section-A (Fig. 7) for the side of $l = 1$ wavelength. This re-

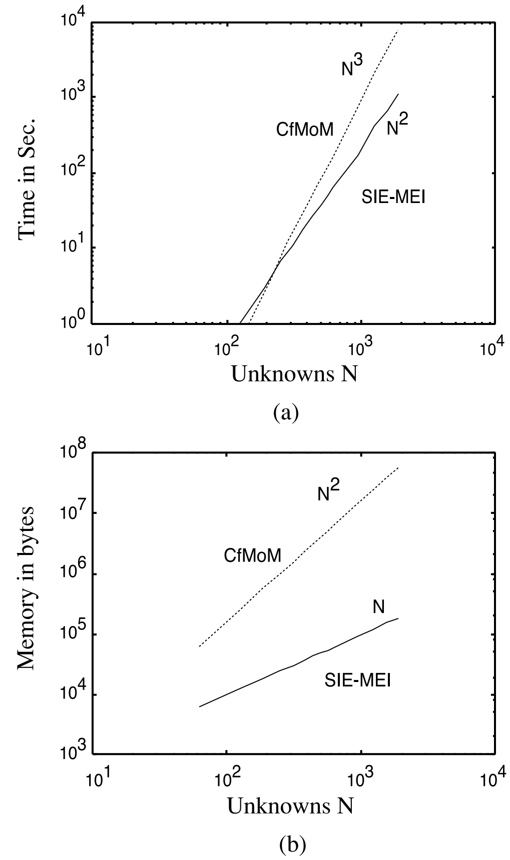

Fig. 10 (a) Total CPU time, and (b) storage memory required by SIE-MEI method and CfMOM.

sult is also compared with the numerical solution using Combined-field Method of Moments (CfMoM)† [15] and gives an excellent agreement between them. As same as sphere, there is some error in the shadowed region, but it does not give any significant effect on the other computation.

5.5 CPU Time and Storage Memory Requirements

In the SIE-MEI method, the surface integral equation is used with the postulates of locality properties. This keeps the advantages of CPU time savings and minimum storage memory requirements as same as MEI [2] and IE-MEI [4] methods. Figure 10 shows the total CPU time (in sec) and storage memory (in bytes) requirements in the SIE-MEI method and compares it with the conventional numerical method (e.g. CfMoM). In both of the cases same parameters are used on a Pentium 533 MHz PC.

In the comparison, total CPU time consists of time required in the integration process to fill the matrix and that for the matrix inversion. In the SIE-MEI method,

†In CfMoM, the internal resonance problem is avoided by using two integral equations, i.e., one for ϕ and the other for $\frac{\partial \phi}{\partial n}$.

time required in the integration precess is $O(QN^2)$ and sparse matrix inversion by using a sparse matrix solver is $O(N)$, respectively, where Q is the number of metrons and N is the integration points on the scatterer surface. On the other hand, for CfMoM the time required in the integration process is $O(N^2)$ and in the matrix inversion is $O(N^3)$. Although, SIE-MEI uses larger CPU time compared to CfMoM for small value of N, this time requirements decreases rapidly as N increases.

For the storage memory requirements, the sparse matrices of SIE-MEI method have the total nonzero elements of matrices $N_t = 2 \times (M \times N)$, where M is the number of nodes in the local region which may be 3, 5, or 9. Since M is very small compared to N and is independent of N, thus in the comparison it can be written as the order of N. Alternatively, the full matrix of CfMoM has the N^2 elements. Thus it is clear that the storage memory requirement of SIE-MEI method is also much smaller than the conventional numerical method.

6. Conclusion

A novel formulation of Scalar-field approach of IE-MEI (SIE-MEI) method for 3D scattering problem is derived from scalar reciprocity relation using 3D scalar Helmholtz equations. The basic concept of this method is the same as IE-MEI method for the 2D electromagnetic wave problem. It reveal that, SIE-MEI method holds the same advantage as minimum memory requirements and CPU time consumption.

The scalar-field approach of IE-MEI with spherical wave function as metron set is one choice. For smooth convergence result, the choice of metrons was also the key to this method. This selection depends on the scatterer geometry. Our proposed method and metron sets are implemented to simple symmetrical shaped body and to arbitrary shaped body and we compare the results with some rigorous and numerical solution. In both of the cases, they have an excellent agreement.

For the body with large dimension and complex structure, the extra care must be taken of the number of metrons, choice of monopole and dipole sources, discretization, etc. To establish our proposed method it is necessary to implement it to other arbitrary shape 3D scalar-field problem and verify the results.

References

[1] K.K. Mei, R. Pous, Z. Chen, Y.W. Liu, and M.D. Prouty, "The measured equation of invariance: A new concept in field computations," IEEE Trans. Antennas & Propag., vol.42, no.3, pp.320–327, March 1994.

[2] R. Pous, The Measured Equation of Invariance: A New Concept in Field Computation, Ph.D. Dissertation, University of California at Berkeley, 1992.

[3] J.M. Rius, "Integral formulation of the measured equation of invariance," Electron. Lett., vol.32, no.1, pp.23–25, Jan. 1996.

[4] J.M. Rius, R. Pous, and A. Cardama, "Integral formulation of the measured equation of invariance: A novel sparse matrix boundary element method," IEEE Trans. Magn., vol.32, no.3, pp.962–967, May 1996.

[5] J.M. Rius, C.P. Carpintero, A. Cardama, and J.R. Mosig, "Theoretical error in the integral equation MEI," Electron. Lett., vol.32, no.23, pp.2131–2132, Nov. 1996.

[6] J.M. Rius, C.P. Carpintero, A. Cardama, and K.A. Michalski, "Analysis of electrically large concave scatterer with the integral equation MEI," Microwave & Optical Technology Letters, vol.14, no.5, pp.287–289, April 1997.

[7] J.M. Rius, C.P. Carpintero, A. Cardama, and J.R. Mosig, "Frequency extrapolation in the integral equation MEI," Electron. Lett., vol.32, no.25, pp.2324–2326, Dec. 1996.

[8] M. Hirose, M. Miyake, J. Takada, and I. Arai, "On the validity of the integral equation formulation of the MEI and the extension to analyze objects with impedance boundary condition," Digest of IEEE AP-S International Symposium, vol.2, pp.1042–1045, June 1998.

[9] M. Hirose, M. Miyake, J. Takada, and I. Arai, "New integral equation formulation of the measured equation of invariance and the extension to analyze two-dimensional cylinders with impedance boundary conditions," Radio Science, vol.34, no.1, pp.65–82, Jan.–Feb. 1999.

[10] M. Hirose, M. Miyake, J. Takada, and I. Arai, "On applicability of the integral equation formulation of the measured equation of invariance to 2D scattering objects," IEICE Trans. Commun., vol.E82-B, no.4, pp.645–654, April 1999.

[11] M. Hirose, J. Takada, and I. Arai, "Analysis of 2-D TE scattering with impedance boundary condition using duality of the IE-MEI method," Proc. ISAP2000, vol.2, pp.733–736, Aug. 2000.

[12] J.M. Rius, J. Parrón, E. Úbeda, and J.R. Mosig, "Integral equation MEI applied to three dimensional arbitrary surfaces," Electron. Lett., vol.33, no.24, pp.2029–2031, Nov. 1997.

[13] J.M. Rius, "Analysis of large and complex antennas by: Multilevel matrix decomposition algorithm (MLMDA) and multilevel fast multipole method (MLFMM)," Presented at National Meeting on Computational Electromagnetics, Laredo, Cantabria, Spain, July 4–6, 2000.

[14] N.M. Alam Chowdhury, J. Takada, and M. Hirose, "An extension of IE-MEI method for 3D acoustic scattering," Tech. Instrumentation and Measurements, IEE Japan, no.IM-01-21, pp.21–26, June 2001.

[15] N. Morita, N. Kumagai, and J.R. Mautz, Integral Equation Methods for Electromagnetics, Artech House, Boston, 1991.

[16] L.N. Trefethen and D. Bau III, Numerical Linear Algebra, Society for Industrial and Applied Mathematics, Philadelphia, 1997.

[17] J.J. Bowman, T.B.A. Senior, and P.L.E. Uslenghi, Electromagnetic and Acoustic Scattering by Simple Shapes, Hemisphere Publishing, New York, 1987.

[18] J.A. Stratton, Electromagnetic Theory, McGraw-Hill, New York, 1941.

N.M. Alam Chowdhury received the B.Sc. Engg. and M.Sc.Engg. degrees in Electrical & Electronic Engg. from Bangladesh Institute of Technology (BIT), Dhaka and Bangladesh University of Engineering & Technology (BUET), Dhaka in 1992 and 1997, respectively. Since May 1992, he has been working in the Dept. of Electrical & Electronic Engg. of BIT Dhaka. Presently he is with the Mobile Communication group of Electrical & Electronic Engg. Dept., Tokyo Institute of Technology (TITech), Tokyo, Japan for pursuing his Ph.D. degree. His research interest includes Electromagnetic Scattering and Radio Wave Propagation. He is a student member of IEEE.

Jun-ichi Takada was born in Tokyo in 1964. He received B.E., M.E. and D.E. degrees from Tokyo Institute of Technology, Japan, in 1987, 1989 and 1992, respectively. From 1992 to 1994, he was a research associate at Chiba University. From 1994, he has been an associate professor at Tokyo Institute of Technology. He received Excellent Paper Award and Young Engineer Award from IEICE Japan in 1993 and 1994, respectively. His current interests are mobile propagation and channel modeling, array signal processing and numerical simulation of waves. He is a member of IEEE, ACES, SIAM and AGU.

Masanobu Hirose was born in Ishikawa Pref., Japan, in 1956. He received a B.S. degree in physics from Kanazawa University, Ishikawa, in 1979, and a M.S. degree in physics from Hiroshima University, Hiroshima, Japan, in 1981, and M.E. and D.E. degrees in electronics engineering from the University of Eectro-Communications, Tokyo, Japan, in 1983 and 1999 respectively. He has been working as a senior researcher in Electromagnetic Waves Division, Metrology Institute of Japan (NMIJ), National Institute of Advanced Industrial Science and Technology (AIST), Ibaraki, Japan since 2000. He is a member of the IEEE.